Multipoint observations of magnetospheric compression-related EMIC Pc1 waves by THEMIS and CARISMA

M. E. Usanova,[1] I. R. Mann,[1] I. J. Rae,[1] Z. C. Kale,[1,2] V. Angelopoulos,[3] J. W. Bonnell,[4] K.-H. Glassmeier,[5] H. U. Auster,[5] and H. J. Singer[6]

[1] Following a long interval (many days) of sustained very quiet geomagnetic conditions, electromagnetic ion cyclotron (EMIC) wave activity was seen by the CARISMA array (www.carisma.ca) on the ground for several hours simultaneously with enhanced solar wind density and related magnetic compression seen at GOES 12 on 29th June 2007. The THEMIS C, D, and E satellites were outbound in a "string-of-pearls" configuration and each observed EMIC waves on L-shells ranging from 5 to 6.5. THEMIS resolved some of the spatial-temporal ambiguity and defined the radial extent of EMIC activity to be ~1.3 Re. The band-limited EMIC waves were seen slightly further out in radial distance by each subsequent THEMIS satellite, but in each case were bounded at high-L by a decrease in density as monitored by spacecraft potential. The EMIC wave activity appears to be confined to a region of higher plasma density in the vicinity of the plasmapause, as verified by ground-based cross-phase analysis. The structured EMIC waves seen at THEMIS E and on the ground have the same repetition period, in contradiction to expectations from the bouncing wave packet hypothesis. Compression-related EMIC waves are usually thought to be preferentially confined to higher L's than observed here. Our observations suggest solar wind density enhancements may also play a role in the excitation of radially localised EMIC waves near the plasmapause. **Citation:** Usanova, M. E., I. R. Mann, I. J. Rae, Z. C. Kale, V. Angelopoulos, J. W. Bonnell, K.-H. Glassmeier, H. U. Auster, and H. J. Singer (2008), Multipoint observations of magnetospheric compression-related EMIC Pc1 waves by THEMIS and CARISMA, *Geophys. Res. Lett.*, *35*, L17S25, doi:10.1029/2008GL034458.

1. Introduction

[2] Pc1 (0.2 to 5 Hz) pulsations are continuous geomagnetic field fluctuations believed to be generated by the electromagnetic ion cyclotron (EMIC) instability, free energy often being provided by equatorial hot ions with temperature anisotropy ($T_{perp} > T_{par}$) [e.g., *Cornwall*, 1965].

[1]Department of Physics, University of Alberta, Edmonton, Alberta, Canada.
[2]Formerly Z. C. Dent.
[3]Department of Earth and Space Sciences, University of California, Los Angeles, USA.
[4]Space Sciences Laboratory, University of California, Berkeley, California, USA.
[5]Institut für Geophysik und Extraterrestrische Physik, Technische Universität Braunschweig, Braunschweig, Germany.
[6]NOAA Space Weather Prediction Center, Boulder, Colorado, USA.

EMIC wave occurrence has been linked to variations in the solar wind flow and interplanetary magnetic field (IMF). In particular, there is a class of dayside Pc1 events that show a strong correlation between EMIC power and increases in solar wind pressure [e.g., *Anderson and Hamilton*, 1993; *Arnoldy et al.*, 2005]. *Olson and Lee* [1983] suggested that magnetospheric compressions cause an increase in hot proton temperature anisotropy. *Anderson and Hamilton* [1993] confirmed that the probability of observing EMIC waves in space increases during magnetospheric compressions, concluding that plasma in the outer dayside magnetosphere is often close to marginal stability such that EMIC waves can be stimulated by even modest compressions. *Anderson et al.* [1992] suggested that the EMIC growth rate, which is inversely proportional to the Alfven velocity ($V_A = B_0/\sqrt{\mu_0 \rho_0}$), peaks at two locations: at high L-shells where the geomagnetic field is relatively weak, and just inside the plasmapause where the ambient plasma density is high. Steep plasmapause density gradients may also provide special propagation conditions that cause local enhancements in growth rates, so that waves can grow significantly even outside the plasmapause, despite the density drop [*Horne and Thorne*, 1993].

[3] *Engebretson et al.* [2002] observed spatially localized EMIC waves, where continuous wave emissions were seen on the ground for extended periods of time. In space, the waves were observed on the Polar satellite for only a few minutes occurring only in radially narrow regions outside the plasmapause from L = 5–11. *Engebretson et al.* [2002] suggested that plasma sheet protons convecting sunward from the nightside magnetosphere were responsible for the EMIC wave generation. Inside the plasmapause, Pc1 activity associated with high solar wind density is more unusual. *Zolotukhina et al.* [2007] reported observations of Pc1-2 waves at low- and high-latitude ground stations during storm recovery phase, suggesting that EMIC activity can be modulated by fast magnetosonic waves launched by the solar wind impacting the magnetopause.

[4] We present coordinated ground-satellite observations of compression-related, dayside, structured [e.g., *Mursula et al.*, 1997] EMIC Pc1 waves from 29th June 2007. The EMIC waves occur coincidentally with a strong solar wind density enhancement following several days of sustained quiet geomagnetic conditions (Kp < 3, Dst > −10 nT). On the ground, structured EMIC wave activity with a wave-packet repetition period of ~3 minutes was observed for several hours simultaneously with the enhancement in solar wind density. In space, the EMIC waves were observed coherently by three THEMIS spacecraft (D, then C, and then E) for a period of 35 minutes as they consecutively crossed the same region of space in a "string-of-pearls"

Figure 1. GSE orbit plot of the trajectories of THEMIS C, D, E (top two panels) between 14:00–16:00 UT; map showing the locations of CARISMA sites and magnetic footprints of THEMIS satellites during the EMIC wave event, starting at 14:35 UT, 14:40 UT and 15:00 UT, respectively (third panel); and GM outbound orbit plot of THEMIS C, D, E superposed over dipole field lines between 14:00–16:00 UT. The EMIC wave event was observed by THEMIS at ~23° magnetic latitude. Thick lines show the locations where each spacecraft observed EMIC waves (THEMIS C and D were so close that their trajectories practically coincide in the figure).

configuration. Multipoint space-ground observations enabled us to determine the location of the waves in the magnetosphere and conclude that the EMIC wave activity was spatially localised, and confined to a region of low spacecraft potential interpreted here as just inside the plasmapause.

2. Observations and Data

[5] The orbits of the five Time History of Events and Macroscale Interactions during Substorms (THEMIS)

[*Sibeck and Angelopoulos*, 2008] spacecraft lined up in a "string-of-pearls" with apogee at 15.4 Re and an orbital period of 36 hours during the initial phase of the mission from launch on February 17 until September 2007. We use data from the THEMIS fluxgate magnetometer (FGM) [*Auster et al.*, 2008] and electric field investigation (EFI) [*Angelopoulos*, 2008] instruments. The Canadian Array for Real-time Investigations of Magnetic Activity (CARISMA; www.carisma.ca) is the continuation and expansion of the CANOPUS magnetometer array. CARISMA has an upgraded cadence (8 samples/s), is expanded through the deployment of new stations, and uses new GPS-timed data loggers and a new data transmission system. The sites used for this study and details of the orbits of THEMIS C, D, and E from 14:00 UT to 16:00 UT are shown in Figure 1.

[6] At around 14:00 UT the onset of a significant solar wind density enhancement ($n = 35$ cm^{-3}), embedded in a slow solar wind ($V = 350$ km/s), arrived at the subsolar magnetopause. This triggered a strong magnetospheric compression that lasted ~4.5 hours. At around 18:00 UT the density dropped back to 10 cm^{-3}, and the solar wind speed increased to around 500 km/s. The amplitude of IMF Bz during the event was 0–4 nT, and the direction remained positive. IMF By was negative (with minimum amplitude being −2 nT) from 14:00 to 15:30 UT. Between 15:30–18:00 UT, By exhibited two short-term negative excursions, remaining predominately positive (<5 nT). The top panel of Figure 2 shows the OMNI [see *King and Papitashvili*, 2005] solar wind dynamic pressure time-shifted to the subsolar magnetopause, as well as the magnetic field magnitude observed by the geosynchronous GOES 12 satellite (10.24° magnetic latitude, 356.90° magnetic longitude). During the solar wind density enhancement GOES 12 was on the dayside between 08:43–13:50 MLT, the magnetic field strength increased by ~35 nT. Coincidently with the compression, and lasting throughout its duration, the ground magnetometers saw clear and long lasting structured EMIC emissions below 0.7 Hz.

[7] In the course of the day, several CARISMA magnetometers registered structured Pc1 activity in the frequency range from 0.3 to 0.7 Hz. Figures 2b–2g show the Fourier spectrograms of the Y-component (geographic east-west) of magnetic field at Fort Churchill (FCHU; L = 7.42), Gillam (GILL; L = 6.13), Island Lake (ISLL; L = 5.13), Pinawa (PINA; L = 4.04), Rabbit Lake (RABB; L = 6.53), and Fort McMurray (MCMU; L = 5.31) from 12:00 to 20:00 UT. Similar waves are also seen in the X-component (geographic north-south). The appearance of structured EMIC emissions by the magnetometers along the ~330° magnetic meridian (also known as the Churchill line; PINA, ISLL, GILL, and FCHU) matches perfectly the beginning of the period of enhanced solar wind density and the associated magnetospheric compression. The most intense structured Pc1 pulsations appear to coincide with peak solar wind densities.

[8] The EMIC wave event discussed here also shows a longitudinal dependence in Pc1 power. The EMIC intensity associated with the early density enhancement (~14:00–16:00 UT) was seen across both the western and Churchill meridian CARISMA sites, while the wave activity from ~17:00–18:00 UT was observed only at the Churchill meridian. The strongest enhancement in EMIC wave power
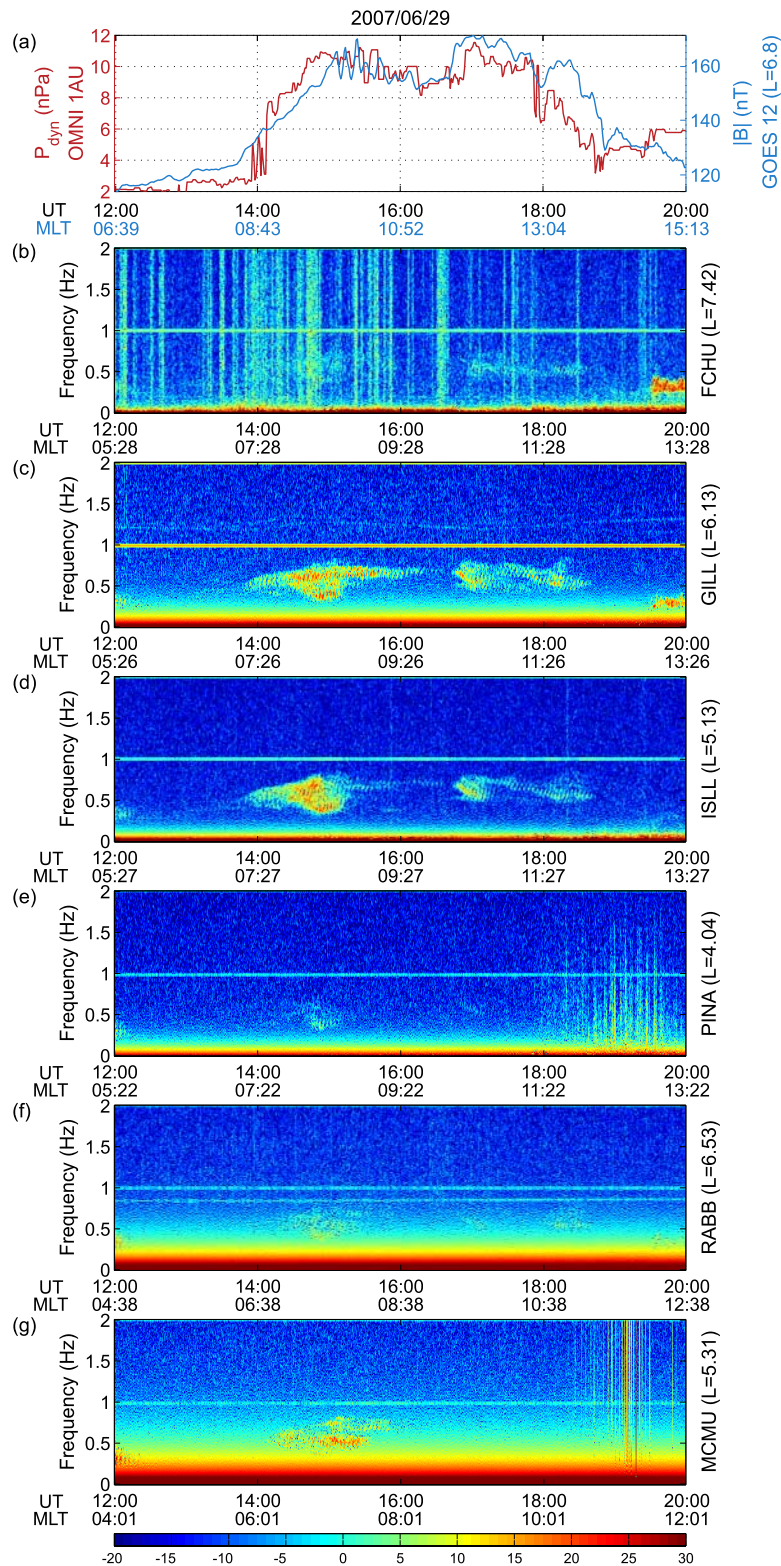
Figure 2. (a) Dynamic solar pressure at 1AU (red line) and the magnitude of the magnetic field observed at GOES 12 (blue line), from 12:00–20:00 UT. (b–g) Fourier spectrograms of the Y-component (geographic east-west) of magnetic field from selected CARISMA stations (see text).

between 14:00–16:00 UT was observed at ISLL (L = 5.13), MCMU (L = 5.31), and GILL (L = 6.13), implying that the waves originated from the vicinity of L = 5–6, before being ducted in the Earth-ionosphere waveguide [e.g., *Fraser*, 1976]. After 19:00 UT, another structured EMIC emission appears (Figures 2b–2c), power being confined to higher-L and at lower frequencies. These lower frequencies are consistent with lower expected ion gyro-frequencies for a

higher-L equatorial source. A similar effect was observed by *Zolotukhina et al.* [2007] during a storm recovery phase, and was attributed in their case to a magnetospheric relaxation.

[9] Figure 3a shows the spectrogram and time-series of the Y-component (geographic east-west) of magnetic field observed at Gillam. Fourier spectrograms of the perpendicular (azimuthal) FGM field in field-aligned coordinates from THEMIS D, C and E are shown in Figures 3b–3d, each THEMIS spectrogram starting at a later time at 14:35 UT, 14:40 UT, and then 15:00 UT, respectively. The EMIC spectrograms show significant similarity from spacecraft to spacecraft, even though these three satellites traverse the same L-shells at progressively later times. Since the EMIC instability is thought to be generated in the equatorial region, it is important to consider how the wave frequency compares to the equatorial ion gyrofrequencies. In order to obtain an equatorial gyrofrequency estimate, the local gyrofrequency was mapped along the field line to the region of minimum B-field with the T96 model [see *Tsyganenko*, 1996] and increased by 27.5 nT, this being the difference between the T96 model and the magnetic field magnitude measured on GOES 12. Each spectrum in Figures 3b–3d shows EMIC power in two distinct frequency bands, separated by a slot region above the estimated equatorial (white line) and below the observed local (black line) helium gyrofrequency. This is believed to indicate the presence of thermal helium in the region of wave excitation [e.g., *Fraser*, 1985].

[10] The red lines in Figures 3b–3d show the EFI spacecraft potential, which can represent a proxy for the ambient electron density, at least in low-density regions [e.g., *Pedersen et al.*, 2001]. Low negative values (more positive values) of floating potentials correspond to the higher (lower) density of surrounding plasma. The spacecraft potential values range between -0.5 to -5 V. These variations in spacecraft potential indicate variations in plasma density and/or temperature and they are interpreted here as due primarily to density changes. The EMIC waves below the equatorial helium gyrofrequency are seen at slightly higher radial distances by each subsequent THEMIS satellite (D, then C, then E), but in each case the EMIC waves appear to be bounded on the high-L side by a similar sharp decrease in potential. The EMIC waves appear to be confined within the high-density (more positive floating potential) side of this potential decrease. Waves above the local helium gyrofrequency appear to be less intense and do not show much correlation with the spacecraft potential. *Horne and Thorne* [1994] found that high plasma densities enable significant wave growth in the bandwidth below the helium gyrofrequency and at the same time reduce the wave gain above the helium gyrofrequency.

[11] In comparison with Figure 3a, we see that only the lower-frequency band is observed simultaneously on the ground. The lack of higher frequency waves on the ground could be due to reflection at the bi-ion frequency, absorption [see *Johnson and Cheng*, 1999], or due to its lower power. Further analysis of the satellite EMIC wave polarization characteristics and Poynting vector is warranted.

[12] Figure 3 also shows the EMIC waveforms filtered between 0.4–0.7 Hz. The EMIC waves observed on the ground from 14:35 to 15:00 UT (see Figure 3a) and on

THEMIS C, D represent wave packets which do not show clear structure. The later (between 15:00–15:35 UT) Pc1 waves appear to be structured both on the ground and on THEMIS E, both having repetition period of about 3 minutes. The amplitude of the waves differs from spacecraft to spacecraft, being ~7 nT on C and E, and ~3 nT on D. The observed amplitude of the waves on the ground is much smaller, about 0.3 nT.

[13] In order to relate the observed structured pulsations to a potential plasmapause location, we used the ground-based magnetometers to determine the local field-line resonance frequencies by applying the cross-phase analysis technique [e.g., *Waters et al.*, 1996] to the data from pairs of CARISMA magnetometers along the ~330° magnetic meridian. Cross-phase FFT windows were 30–50 minutes long, taken between 15:00–16:00 UT. Plasma mass densities were derived from the field-line resonance frequencies assuming a dipole field geometry and radial density distribution along field lines $\sim r^{-3}$ [see *Dent et al.*, 2003]. The resonance frequency and plasma mass density profiles show that a steep plasmapause was located between L = 4.53 and 5.60, identified by the region of positive frequency gradient and steepening density gradient [e.g., *Kale et al.*, 2007]. Corresponding T96 field lines map to a geocentric apex location between 4.84 and 5.94 Re, while the density gradient was encountered by the spacecraft between 6.21 and 6.42 Re. The discrepancy between the field line apex plasmapause location estimated from the ground and satellite observations could be caused by quiet time structure of the plasmapause [*Carpenter and Anderson*, 1992] or be due to uncertainties in magnetic field line mapping. The regions where each of the THEMIS satellites saw EMIC waves below the equatorial helium gyrofrequency are shown in Figure 3e. The separation between the spacecraft remained ~0.1 R_e between THEMIS D and C, and ~0.5 R_e between C and E. EMIC waves were coherently recorded by the THEMIS D, C and E in localized emissions with a width of ~1.3 Re. The region supporting the Pc1 pulsations moved outwards slightly from the time of the crossing of THEMIS C and E, however the waves spanned the range of T96 geocentric apex location of 4.96 to 6.21 Re which is consistent with the ground-based observations.

3. Conclusions

[14] We have presented simultaneous ground-satellite observations of structured dayside Pc1 emissions related to magnetospheric compressions arising from enhanced densities in the solar wind. In space, the EMIC emissions appeared in two frequency bands both below and above the local helium gyrofrequency, with a clear slot region in emissions. Using three THEMIS satellites, we were able to clearly resolve the spatio-temporal ambiguity to show that the EMIC emissions below the equatorial helium gyrofrequency were radially localized to a region ~1.3 Re wide.

[15] The waves below the equatorial helium gyrofrequency were confined at higher-L by a sharp decrease in spacecraft potential indicating their apparent confinement within a region of higher plasma density. The most intense waves on the ground were observed at the same L and the same frequency as those in space; however, only waves in
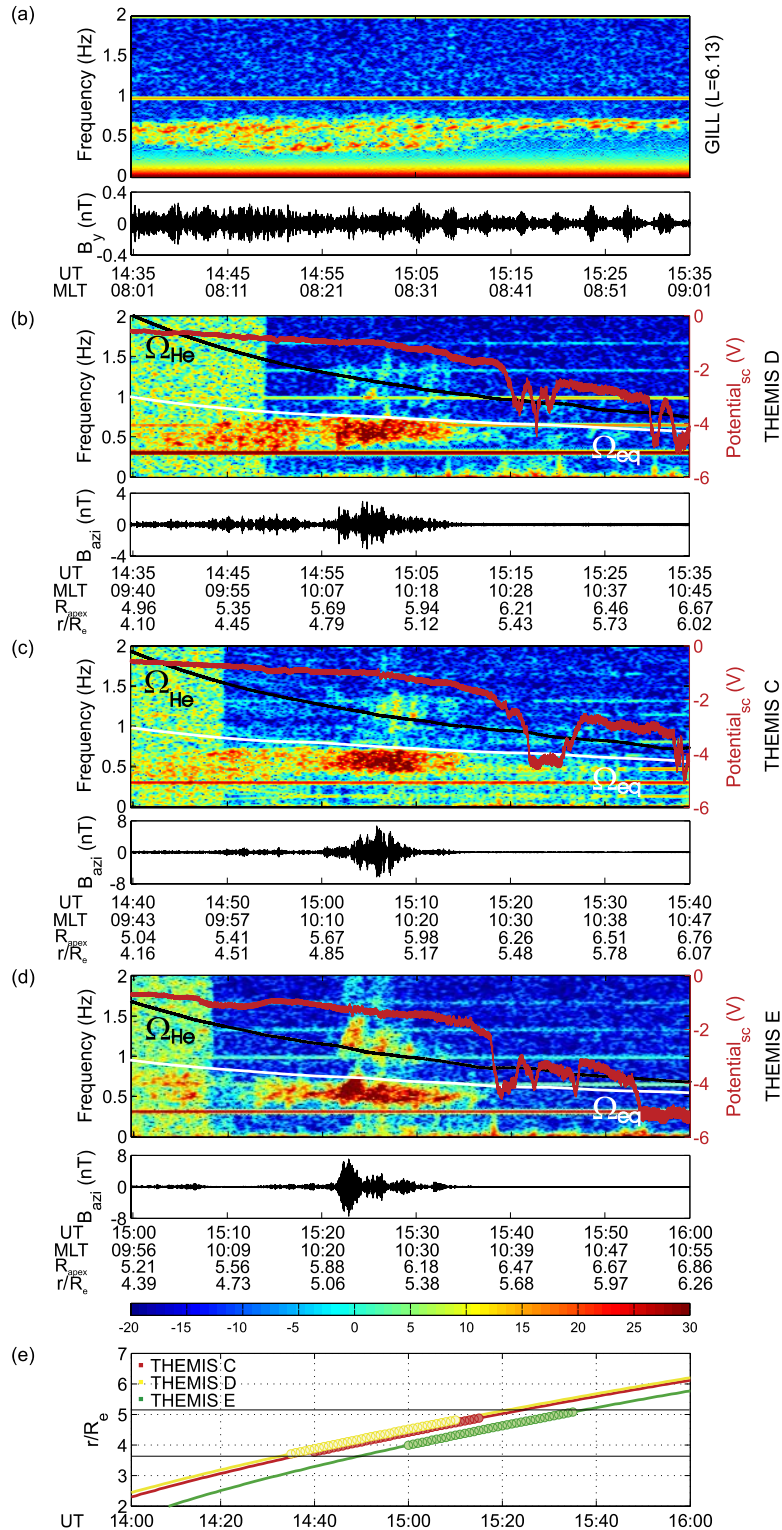
Figure 3. (a) (top) Fourier spectrogram and (bottom) time-series of the Y-component (geographic east-west) of magnetic field at Gillam. (b–d) (top) Fourier spectral density and (bottom) waveforms of the perpendicular (azimuthal) magnetic field component in field-aligned coordinates for one hour windows at THEMIS D, C, and E, starting at 14:35 UT, 14:40 UT and 15:00 UT, respectively (the change in background color from green to blue corresponds to the range change of the FGM); over-plotted are the spin-plane spacecraft potential (red line), the local (black line) and the equatorial (white line) helium gyrofrequency. The apexes of the geomagnetic field lines (see x-labels) were obtained by tracing field lines from THEMIS to the minimum |B| using the T96 model. (e) Geocentric radial distance of THEMIS C, D and E as a function of UT. Thick lines show the intervals where each spacecraft sees EMIC waves.

the lower frequency band below the equatorial helium gyrofrequency were observed on the ground. The repetition period of structured Pc 1 waves on the ground and on THEMIS E was also found to be almost the same, which cannot be explained by the bouncing wave packet model [e.g., *Jacobs and Watanabe*, 1964]. Ground-based cross-phase estimates of the plasmapause location also place the EMIC waves close to the plasmapause region in space which is thought to provide a preferential region for wave growth through convective amplification and gain [e.g., *Horne and Thorne*, 1993] and where the structured Pc1 pulsations are typically observed [e.g., *Mursula et al.*, 1997]. Structure in the boundary layer of the quiet time plasmapause [*Carpenter and Anderson*, 1992] could also explain different wave excitation conditions and hence the different wave amplitudes seen during the sequential pass of each THEMIS satellite.

[16] Usually, compression-related EMIC waves are thought to be preferentially confined to higher-L regions closer to the magnetopause during compressions at quiet times [see *Engebretson et al.*, 2002] and only inside or close to the plasmapause during the recovery phase of storms, following ion injections. Our observations suggest solar wind density enhancements and magnetospheric compressions may also be an important source for lower-L radially confined EMIC emissions close to the plasmapause, perhaps due to enhanced temperature anisotropy which develops along dayside ion drift trajectories in a compressed magnetosphere. Given the potential role for EMIC waves in MeV electron loss in the radiation belts [e.g., *Summers and Thorne*, 2003], and the correlation between the plasmapause and the inner edge of the outer zone electron radiation belt [e.g., *Li et al.*, 2006], these observations may have wider importance for inner magnetosphere energetic particle dynamics.

References

Anderson, B. J., and D. J. Hamilton (1993), Electromagnetic ion cyclotron waves stimulated by modest magnetospheric compressions, *J. Geophys. Res.*, 98, 11,369–11,382.

Anderson, B. J., R. E. Erlandson, and L. J. Zanetti (1992), A statistical study of Pc 1–2 magnetic pulsations in the equatorial magnetosphere: 1. Equatorial occurrence distribution, *J. Geophys. Res.*, 97, 3075–3088.

Angelopoulos, V. (2008), The THEMIS mission, *Space Sci. Rev.*, in press.

Arnoldy, R. L., et al. (2005), Pc 1 waves and associated unstable distributions of magnetospheric protons observed during a solar wind pressure pulse, *J. Geophys. Res.*, 110, A07229, doi:10.1029/2005JA011041.

Auster, H. U., et al. (2008), The THEMIS fluxgate magnetometer, *Space Sci. Rev.*, in press.

Carpenter, D., and R. Anderson (1992), Whistler model of equatorial electron density in the magnetosphere, *J. Geophys. Res.*, 97, 1097–1108.

Cornwall, J. M. (1965), Cyclotron instabilities and electromagnetic emissions in the ultra low frequency and very low frequency ranges, *J. Geophys. Res.*, 70, 61–69.

Dent, Z. C., I. R. Mann, F. W. Menk, J. Goldstein, C. R. Wilford, M. A. Clilverd, and L. G. Ozeke (2003), A coordinated ground-based and IMAGE satellite study of quiet-time plasmaspheric density profiles, *Geophys. Res. Lett.*, 30(12), 1600, doi:10.1029/2003GL016946.

Engebretson, M. J., W. K. Peterson, J. L. Posch, M. R. Klatt, B. J. Anderson, C. T. Russell, H. J. Singer, R. L. Arnoldy, and H. Fukunishi (2002), Observations of two types of Pc 1–2 pulsations in the outer dayside magnetosphere, *J. Geophys. Res.*, 107(A12), 1451, doi:10.1029/2001JA000198.

Fraser, B. J. (1976), Pc1 geomagnetic pulsation source regions and ionospheric waveguide propagation, *J. Atmos. Terr. Phys.*, 38, 1141–1146.

Fraser, B. J. (1985), Observations of ion cyclotron waves near synchronous orbit and on the ground, *Space Sci. Rev.*, 42, 357–374.

Horne, R. B., and R. M. Thorne (1993), On the preferred source location for the convective amplification of ion cyclotron waves, *J. Geophys. Res.*, 98, 9233–9247.

Horne, R. B., and R. M. Thorne (1994), Convective instabilities of electromagnetic ion cyclotron waves in the outer magnetosphere, *J. Geophys. Res.*, 99, 17,259–17,273.

Jacobs, J. A., and T. Watanabe (1964), Micropulsation whistlers, *J. Atmos. Sol. Terr. Phys.*, 26, 825–829.

Johnson, J. R., and C. Z. Cheng (1999), Can ion cyclotron waves propagate to the ground?, *Geophys. Res. Lett.*, 26(6), 671–674.

King, J. H., and N. E. Papitashvili (2005), Solar wind spatial scales in and comparisons of hourly Wind and ACE plasma and magnetic field data, *J. Geophys. Res.*, 110, A02104, doi:10.1029/2004JA010649.

Kale, Z. C., I. R. Mann, C. L. Waters, J. Goldstein, F. W. Menk, and L. G. Ozeke (2007), Ground magnetometer observation of a cross-phase reversal at a steep plasmapause, *J. Geophys. Res.*, 112, A10222, doi:10.1029/2007JA012367.

Li, X., D. N. Baker, T. P. O'Brien, L. Xie, and Q. G. Zong (2006), Correlation between the inner edge of outer radiation belt electrons and the innermost plasmapause location, *Geophys. Res. Lett.*, 33, L14107, doi:10.1029/2006GL026294.

Mursula, K., R. Rasinkangas, T. Bösinger, R. Erlandson, and P.-A. Lindqvist (1997), Nonbouncing Pc 1 wave bursts, *J. Geophys. Res.*, 102, 17,611–17,624.

Olson, J. V., and L. C. Lee (1983), Pc1 wave generation by sudden impulses, *Planet. Space Sci.*, 31, 295–302.

Pedersen, A., et al. (2001), Four-point high time resolution information on electron densities by the electric field experiments (EFW) on Cluster, *Ann. Geophys.*, 19, 1483–1489.

Sibeck, D. G., and V. Angelopoulos (2008), THEMIS science objectives and mission phases, *Space Sci. Rev*, in press.

Summers, D., and R. M. Thorne (2003), Relativistic electron pitch-angle scattering by electromagnetic ion cyclotron waves during geomagnetic storms, *J. Geophys. Res.*, 108(A4), 1143, doi:10.1029/2002JA009489.

Tsyganenko, N. A. (1996), Effects of the solar wind conditions on the global magnetospheric configuration as deduced from data-based field models, in *Proceedings of the ICS-3 Conference on Substorms*, edited by E. J. Rolfe and B. Kaldeich, *Eur. Space Agency Spec. Publ.*, ESA SP-389, 181–185.

Waters, C. L., J. C. Samson, and E. F. Donovan (1996), Variation of plasmatrough density derived from magnetospheric field line resonances, *J. Geophys. Res.*, 101, 24,737–24,745.

Zolotukhina, N., et al. (2007), Response of the inner and outer magnetosphere to solar wind density fluctuations during the recovery phase of a moderate magnetic storm, *J. Atmos. Sol. Terr. Phys.*, 69, 1707–1722.

————————————

V. Angelopoulos, Department of Earth and Space Sciences, University of California, Los Angeles, CA 90095-1567, USA.

H. U. Auster and K.-H. Glassmeier, Institut für Geophysik und Extraterrestrische Physik, Technische Universität Braunschweig, Mendelssohnstrasse 3, D-38106 Braunschweig, Germany.

J. W. Bonnell, Space Science Laboratory, University of California, Berkeley, CA 94720, USA.

Z. C. Kale, I. R. Mann, I. J. Rae, and M. E. Usanova, Department of Physics, University of Alberta, Edmonton, AB T6G 2G7, Canada. (musanova@phys.ualberta.ca)

H. J. Singer, NOAA Space Weather Prediction Center, Boulder, CO 80303, USA.